Supporting Information

Methoxy Substituents Activated Carbazole-Based Boron Dimesityl TADF Emitters

Paramaguru Ganesan,[a,†] Deng-Gao Chen,[b,†] Wen-Cheng Chen,[c] Jia-An Lin,[b] Chun-Ying Huang,[b] Meng-Chi Chen,[b] Chun-Sing Lee,*[,c] Pi-Tai Chou,*[,b] and Yun Chi,*[,a,d]

[a] Department of Chemistry and Frontier Research Center on Fundamental and Applied Sciences of Matters, National Tsing Hua University, Hsinchu 30013, Taiwan

[b] Department of Chemistry, National Taiwan University, Taipei 10617, Taiwan

[c] Center of Super-Diamond and Advanced Films (COSDAF) and Department of Chemistry, City University of Hong Kong, Hong Kong SAR.

[d] Department of Chemistry and Department of Materials Science and Engineering, City University of Hong Kong, Hong Kong SAR

[†]These authors contributed equally

Corresponding Author

Chun-Sing Lee, E-mail: apcslee@cityu.edu.hk

Pi-Tai Chou, E-mail: chop@ntu.edu.tw

Yun Chi, E-mail: yunchi@cityu.edu.hk

Keywords: boron, carbazole, charge transfer, TADF, OLEDs

Table of Contents

1. Experimental Section S3-4

2. Experimental procedures S5-11

Scheme S1. Synthetic routes of (A) Cz-1 and Cz-2 and (B) Cz-3 ..... S10

Scheme S2. Synthetic routes of **CzBM-1**, **2** and **3** and **CzPBM-2** and **3** S10

Figure S1. ^{1}H NMR of **CzBM-3** and **CzPBM-3**. S11

3. Thermogravimetric analysis (TGA) Methods S12

Figure S2. TGA (left) and DSC (right) data of **CzBM-1** to **3**, **CPBM-2** and **3** S12

Table S1. Thermal analysis of **CzBM-1** to **3**, **CPBM-2** and **3** S12

4. Photophysical properties S13-16

Figure S3. The time resolved PL spectra of the titled molecules in CH_2Cl_2 ..... S13

Figure S4. Transient photoluminescence characteristics of the **CzBM-1** S14

Figure S5. Transient photoluminescence characteristics of the **CzBM-2** S14

Figure S6. Transient photoluminescence characteristics of **CzBM-3** S14

Figure S7. Transient photoluminescence characteristics of **CzPBM-2** and **3** S15

Figure S8. Transient photoluminescence characteristics of neat films S15

Table S2. Photophysical properties of the studied boron compounds. S16

5. Cyclic Voltammograms studies S17

Figure S9. Cyclic voltammograms of Cz-2 and Cz-3, **CzBM-1** to **3**, and **CPBM-2** and **3** S17

Table S3. Electrochemical properties and calculated bandgaps of the TADF molecules S17

6. Computational approaches S18-21

Table S4 to **S5** Calculated wavelength and orbital transition analyses for **CzBM-1** S18

Table S6 to **S7** Calculated wavelength and orbital transition analyses for **CzBM-2** S18

Table S8 to **S9** Calculated wavelength and orbital transition analyses for **CzBM-3** S19

Table S10 Calculated wavelength and orbital transition analyses for **CzPBM-0** S19

Table S11 to **S12** Calculated wavelength and orbital transition analyses for **CzPBM-2** S20

Table S13 to **S14** Calculated wavelength and orbital transition analyses for **CzPBM-3** S21

Table S15. Calculated orbital energy levels' for the titled molecules S21

1. Experimental Section

General Procedures. Solvents were dried over appropriate drying agents and commercially available reagents were used without further purification. All reactions were conducted under nitrogen atmosphere unless otherwise noted. All reactions were monitored by pre-coated TLC plates (0.20 mm with fluorescent indicator F_{254}). Mass spectra were obtained on a JEOL SX-102A instrument operating in electron impact (EI) or fast atom bombardment (FAB) mode. The ^{1}H, and ^{13}C NMR spectra were recorded on a Varian Mercury-400 or an INOVA-500 instrument. Elemental analysis was carried out with a Heraeus CHN-O-Rapid Elemental Analyzer. Thermal analysis was performed using a Seiko Instrument TG/DTA 320 thermogravimetric analyzer at a heating rate of 10 °C/min and under nitrogen. Differential scanning calorimeter (DSC) was conducted using a Seiko Instrument DSC220C, with a heating and cooling rate of 10 °C /min.

Photophysical Characterization: Steady-state absorption spectra were recorded using a Hitachi U-3310 spectrophotometer, and emission spectra were obtained using an Edinburgh FS920 fluorimeter. Time-resolved PL (PL decay curves) was measured by monitoring the decay of the intensity at the PL peak wavelength using the time-correlated single-photon counting (TCSPC) technique and nanosecond pulsed light excitation from a pulsed hydrogen-filled lamp (355 nm), with a fluorescence lifetime system (Edinburgh FLS920).

Single Crystal X-Ray Diffraction Studies: Single crystal X-ray diffraction data were measured on a Bruker SMART Apex CCD diffractometer using Mo radiation (λ = 0.71073 Å). The data collection was executed using the *SMART* program. Cell refinement and data reduction were performed with the *SAINT* program. An empirical absorption was applied based on the symmetry-equivalent reflections and the *SADABS* program. The structures were solved using the *SHELXS-97* program and refined using *SHELXL-97* program by full-matrix least squares on F^2 values. CCDC-1900690, 1900691, and 1900692 contains the supplementary crystallographic data of **CzBM-1**, **CzBM-3** and **CzPBM-3** respectively. The data can be obtained free of charge from the Cambridge Crystallographic Data Centre via http://www.ccdc.cam.ac.uk

Computational Methods: The geometries of the ground state for the titled compounds were optimized by the density functional theory (DFT) method. The electronically excited-state structures with relevant photophysical properties were calculated by the time-dependent density functional theory (TD-DFT) method with a M062X hybrid function in combination with a polarizable continuum model (PCM). The 6-31+G(d,p) basis set was employed for all atoms. All theoretical calculations were performed using the Gaussian 09 program.

OLED Fabricated Methods: OLEDs were fabricated on cleaned ITO-coated glass substrates as anode with a sheet resistance of 15 Ω square^{-1}. Before use, ITO substrates were swabbed with diluted Decon-90 solution. After 20-min ultrasonic bath in acetone and deionized water respectively, and the substrates were then rinsed with isopropanol. Dry nitrogen flow was used to remove the surface on the surface, and then the substrates were stored in an oven at 100 °C. After a 20-minute UV/O_3 cleaning, the ITO substrates were transfer into a vacuum chamber (~10^{-6} torr) for material deposition. Electrical characteristics of devices were measured by a Keithley 237 power source, while electroluminescence properties were recorded on a Spectrascan PR650 photometer. OLED measurements were conducted under ambient condition without any encapsulation.

2. Experimental procedures

Synthesis of **5**: 2-bromoaniline (2.00 g, 11.63 mmol), 2-methoxyiodobenzene (2.99 g, 12.78 mmol), $Pd_2(dba)_3$ (0.11 g, 0.12 mmol), bis(diphenylphosphino)ferrocene (0.13 g, 0.23 mmol) and ^{t}BuONa (1.68 g, 17.44 mmol) were dissolved in toluene (80 mL) and then the solution was heated to reflux. After being stirred for 24 hours, the mixture was cooled to room temperature and partitioned between water and ethyl acetate. The organic layer was separated and the aqueous layer was extracted with ethyl acetate (2 × 50 mL). The combined organic layers were washed with brine, dried over Na_2SO_4, and concentrated to dryness. The resulting residue was purified by silica gel column chromatography, eluting with hexane and ethyl acetate (99:1) to afford **5** as yellow liquid (2.15 g, 66 %). The derivatives **6** and **9** were obtained according to the same procedure as described above.

Spectral Data of **5**: ^{1}H NMR (400 MHz, acetone, 298 K): δ 7.58 (d, *J* = 8.0 Hz, 1H), 7.35 – 7.21 (m, 3H), 7.06 (d, *J* = 8.0 Hz, 1H), 6.98 (t, *J* = 7.7 Hz, 1H), 6.91 (t, *J* = 7.6 Hz, 1H), 6.81 (dd, *J* = 8.3, 6.8 Hz, 1H), 6.55 (bs, 1H), 3.91 (s, 3H). MS (FAB), *m/z* 277.0 [M^+].

Spectral Data of **6**: ^{1}H NMR (400 MHz, $CDCl_3$, 298 K): δ 7.30 (d, *J* = 7.9 Hz, 1H), 7.20 (d, *J* = 8.6 Hz, 1H), 7.10 – 7.00 (m, 2H), 6.75 – 6.66 (m, 1H), 6.54 (d, *J* = 2.7 Hz, 1H), 6.46 (dd, *J* = 8.6, 2.7 Hz, 1H), 6.06 (bs, 1H), 3.82 (s, 3H), 3.80 (s, 3H). MS (FAB), *m/z* 263.1 [M^+].

Spectral Data of **9**: ^{1}H NMR (400 MHz, $CDCl_3$, 298 K): δ 7.12 (d, *J* = 8.7 Hz, 2H), 7.03 (d, *J* = 7.5 Hz, 1H), 6.92 – 6.83 (m, 3H), 6.83 – 6.71 (m, 2H), 5.97 (bs, 1H), 3.90 (s, 3H), 3.80 (s, 3H). MS (FAB), *m/z* 229.1 [M^+].

Synthesis of **Cz-1**: To a mixture of **5** (1.60 g, 5.75 mmol), potassium carbonate (1.59 g, 11.50 mmol), $Pd(OAc)_2$ (0.13 g, 0.57 mmol) and $P(^tBu)_3{\cdot}HBF_4$ (0.33 g, 1.15 mmol) was added dimethylacetamide (40 mL) and toluene (40 ml) under N_2 atmosphere. The reaction mixture was heated to reflux and being stirred for 24 hours, the mixture was cooled to room temperature and partitioned between water and ethyl acetate. The organic layer was separated and the aqueous layer was extracted with ethyl acetate (2 × 100 mL). The combined organic layers were washed with brine, dried over Na_2SO_4, and concentrated to dryness. The resulting residue was purified by silica gel column chromatography, eluting with hexane and ethyl acetate (99:1) to afford **Cz-1** as white powder (0.64 g, 56 %). **Cz-2** was obtained according to the same procedure as described above.

Spectral Data of **Cz-1**: ^{1}H NMR (400 MHz, acetone, 298 K): δ 10.31 (bs, 1H), 8.06 (d, *J* = 7.9 Hz, 1H), 7.68 (d, *J* = 7.8 Hz, 1H), 7.56 (d, *J* = 8.2 Hz, 1H), 7.36 (t, *J* = 7.6 Hz, 1H), 7.15 (ddd, *J* = 8.0, 7.1, 1.0 Hz, 1H), 7.10 (t, *J* = 7.8 Hz, 1H), 6.95 (d, *J* = 7.8 Hz, 1H), 3.99 (s, 3H). MS (EI), *m/z* 197.1 [M^+].

Spectral Data of **Cz-2**: ^{1}H NMR (400 MHz, $CDCl_3$, 298 K): δ 8.09 (bs, 1H), 7.99 (d, *J* = 8.0 Hz, 1H), 7.46 – 7.32 (m, 2H), 7.18 (t, *J* = 7.4 Hz, 1H), 7.11 (d, *J* = 2.0 Hz, 1H), 6.58 (d, *J* = 2.0 Hz, 1H), 3.97 (s, 3H), 3.92 (s, 3H). MS (EI), *m/z* 227.1 [M^+].

Synthesis of **Cz-3**: To a mixture of **9** (4.00 g, 17.44 mmol), potassium carbonate (0.24 g, 0.87 mmol), and $Pd(OAc)_2$ (0.20 g, 0.89 mmol) was added pivalic acid (50 mL) under open air condition. The reaction mixture was heated to 130 °C and, after stirring overnight, the mixture was cooled to room temperature and partitioned between water and ethyl acetate. The organic layer was separated and the aqueous layer was extracted with ethyl acetate (2 × 100 mL). The combined organic layers were washed with brine, dried over Na_2SO_4, and concentrated to dryness. The resulting residue was purified by silica gel column chromatography, eluting with hexane and ethyl acetate (4:1) to afford **Cz-3** as light yellow powder (2.60 g, 66 %).

Spectral Data of **Cz-3**: ^{1}H NMR (400 MHz, $CDCl_3$, 298 K): δ 8.10 (bs, 1H), 7.62 (d, *J* = 7.9 Hz, 1H), 7.51 (d, *J* = 1.5 Hz, 1H), 7.34 (d, *J* = 8.7 Hz, 1H), 7.12 (t, *J* = 7.8 Hz, 1H), 7.05 (d, *J* = 6.3 Hz, 1H), 6.87 (d, *J* = 7.8 Hz, 1H), 3.99 (s, 3H), 3.91 (s, 3H). MS (EI), *m/z* 227.1 [M^+].

Synthesis of **CzBM-1**: To a solution of **Cz-1** (0.50 g, 2.53 mmol) in THF (10 mL) was slowly added 1.1 mL of 2.5 M solution of *n*-BuLi in hexane at −78 °C and stirred for 2 h. After that, dimesitylfluoroborane (1.02 g, 3.8 mmol) in THF (10 mL) was added, and was gradually warmed up to room temperature over 4 h and then heated to reflux for another 12 h. The resulting reaction mixture was quenched with water (20 mL) and extracted with ethyl acetate (2 × 50 mL). The combined organic layers were washed with brine, dried over Na_2SO_4, and concentrated to dryness. The resulting residue was purified by silica gel column chromatography, eluting with hexane and CH_2Cl_2 (10:1) to afford **CzBM-1** as white powder (0.57 g, 51 %). Compounds **CzBM-2** and **CzBM-3** were prepared by following the procedure described for **CzBM-1**.

Spectral Data of **CzBM-1**: ^{1}H NMR (400 MHz, $CDCl_3$, 298 K): δ 7.97 (d, *J* = 7.5 Hz, 1H), 7.62 (d, *J* = 7.6 Hz, 1H), 7.23 (dd, *J* = 16.1, 8.5 Hz, 2H), 7.10 (t, *J* = 7.6 Hz, 1H), 6.87 (s, 2H), 6.84 (s, 1H),

6.78 (s, 1H), 6.73 (d, J = 7.9 Hz, 1H), 6.51 (s, 1H), 3.27 (s, 3H), 2.36 (s, 3H), 2.35 (s, 3H), 2.22 (s, 3H), 2.16 (s, 3H), 1.92 (s, 3H), 1.27 (s, 3H). ^{13}C NMR (100 MHz, $CDCl_3$): δ 149.40, 141.97, 141.80, 141.29, 139.67, 139.42, 137.96, 133.51, 130.50, 129.00, 128.68, 128.39, 128.04, 127.86, 126.65, 123.32, 121.87, 119.96, 114.52, 111.99, 108.49, 54.58, 23.01, 22.71, 21.82, 21.56, 20.78. MS (FAB): m/z 445.3 [M^+]. Anal. Calcd. for $C_{31}H_{32}N$: C, 83.59; H, 7.24; N, 3.14. Found: C, 83.40; H, 7.38; N, 3.05.

Spectral Data of **CzBM-2**: ^{1}H NMR (400 MHz, $CDCl_3$, 298 K): δ 7.93 (d, J = 7.8 Hz, 1H), 7.19 (t, J = 7.4 Hz, 1H), 7.08 (s, 1H), 7.05 (d, J = 7.3 Hz, 1H), 6.88 (s, 2H), 6.80 (d, J = 8.5 Hz, 2H), 6.54 (bs, 1H), 6.36 (s, 1H), 3.89 (s, 3H), 3.24 (s, 3H), 2.35 (s, 3H), 2.31 (bs, 3H), 2.21 (s, 3H), 2.13 (bs, 3H), 1.89 (bs, 3H), 1.27 (bs, 3H).^{13}C NMR (100 MHz, $CDCl_3$): δ 156.60, 149.69, 143.40, 141.52, 140.97, 139.41, 139.00, 137.53, 130.19, 128.69, 128.34, 128.08, 127.71, 126.35, 121.42, 119.44, 114.39, 98.35, 93.45, 55.76, 54.37, 22.64, 22.33, 21.51, 21.26, 20.52. MS (FAB): m/z 475.3 [M^+]. Anal. Calcd. for $C_{32}H_{34}N$: C, 80.84; H, 7.21; N, 2.95. Found: C, 81.03; H, 6.99; N, 3.11.

Spectral Data of **CzBM-3**: ^{1}H NMR (400 MHz, $CDCl_3$, 298 K): δ 7.56 (dd, J = 7.7, 0.9 Hz, 1H), 7.42 (t, J = 1.5 Hz, 1H), 7.19 (t, J = 7.8 Hz, 1H), 6.86 (s, 2H), 6.77 (s, 1H), 6.71 (t, J = 3.3 Hz, 3H), 6.51 (s, 1H), 3.87 (s, 3H), 3.25 (s, 3H), 2.35 (s, 3H), 2.33 (s, 3H), 2.21 (s, 3H), 2.15 (s, 3H), 1.91 (s, 3H), 1.29 (s, 3H). ^{13}C NMR (100 MHz, $CDCl_3$): δ 155.28, 149.51, 141.85, 141.28, 139.65, 139.31, 137.83, 137.77, 134.14, 130.50, 129.01, 128.99, 128.99, 128.65, 128.35, 128.00, 123.15, 115.37, 114.84, 111.91, 108.51, 102.98, 56.01, 54.54, 22.97, 22.62, 21.80, 21.56, 20.80. MS (FAB): m/z 475.3 [M^+]. Anal. Calcd. for $C_{32}H_{34}N$: C, 80.84; H, 7.21; N, 2.95. Found: C, 81.04; H, 7.08; N, 3.00.

Synthesis of **13**: A flask containing Cz-2 (1.00 g, 4.40 mmol), 1-bromo-4-iodobenzene (2.49 g, 8.80 mmol), potassium carbonate (1.82 g, 13.20 mmol) and copper powder (0.84 g, 13.20 mmol) was evacuated and backfilled with nitrogen. Degassed DMF was added and the reaction mixture was heated to reflux and continued to stir for 12 h. It was next cooled to RT, filtered via Celite, washed with ethyl acetate and partitioned between water and ethyl acetate. The organic layer was separated and the aqueous layer was extracted with ethyl acetate (2 × 100 mL). The combined organic layers were washed with brine, dried over Na_2SO_4, and concentrated to dryness. The resulting residue was purified by silica gel column chromatography, eluting with hexane and ethyl acetate (10:0.2) to afford **13** as

white powder (1.39 g, 83 %). Compound **14** was prepared by following the procedure described for **13**.

Spectral Data of **13**: ^{1}H NMR (400 MHz, $CDCl_3$, 298 K): δ 7.69 (d, *J* = 7.8 Hz, 1H), 7.58 (d, *J* = 8.7 Hz, 2H), 7.53 (d, *J* = 2.4 Hz, 1H), 7.29 (d, *J* = 8.7 Hz, 2H), 7.17 (t, *J* = 7.8 Hz, 2H), 7.10 (d, *J* = 8.9 Hz, 1H), 6.99 (dd, *J* = 8.9, 2.5 Hz, 1H), 6.88 (d, *J* = 7.9 Hz, 1H), 3.91 (s, 3H), 3.68 (s, 3H). MS(EI), *m/z* 381.1 [M^+].

Spectral Data of **14**: ^{1}H NMR (400 MHz, $CDCl_3$, 298 K): δ 8.03 (d, *J* = 7.8 Hz, 1H), 7.59 (d, *J* = 8.5 Hz, 2H), 7.38 – 7.31 (m, 2H), 7.29 (d, *J* = 8.4 Hz, 2H), 7.22 (d, *J* = 6.3 Hz, 1H), 7.18 (d, *J* = 2.2 Hz, 1H), 6.57 (d, *J* = 2.1 Hz, 1H), 3.94 (s, 3H), 3.67 (s, 3H). MS (EI), *m/z* 381.1 [M^+].

Synthesis of **CzPBM-2**: To a solution of **13** (1.00 g, 2.62 mmol) in THF (30 mL) was slowly added 1.15 mL of 2.5 M solution of *n*-BuLi in hexane at −78 °C and stirred for 2 h. After that, dimesitylfluoroborane (1.05 g, 3.92 mmol) in THF (10 mL) was added, and was gradually warmed up to room temperature and stirred for 12 h. The resulting reaction mixture was quenched with water (20 mL) and extracted with ethyl acetate (2 × 50 mL). The combined organic layers were washed with brine, dried over Na_2SO_4, and concentrated to dryness. The resulting residue was purified by silica gel column chromatography, eluting with hexane and CH_2Cl_2 (10:1) to afford **CzPBM-2** as light yellow powder (0.69 g, 48 %). Compound **CzPBM-3** was prepared by following the procedure described for **CzPBM-2**.

Spectral Data of **CzPBM-2**: ^{1}H NMR (400 MHz, $CDCl_3$, 298 K): δ 8.05 (d, *J* = 7.8 Hz, 1H), 7.63 (d, *J* = 7.8 Hz, 2H), 7.40 (d, *J* = 7.8 Hz, 2H), 7.36 (d, *J* = 7.1 Hz, 1H), 7.30 (d, *J* = 7.8 Hz, 1H), 7.23 (d, *J* = 7.0 Hz, 1H), 7.20 (d, *J* = 2.1 Hz, 1H), 6.87 (s, 4H), 6.59 (d, *J* = 2.0 Hz, 1H), 3.96 (s, 3H), 3.64 (s, 3H), 2.34 (s, 6H), 2.11 (s, 12H). ^{13}C NMR (100 MHz, $CDCl_3$): δ 155.06, 147.52, 142.69, 142.02, 140.96, 138.90, 136.51, 128.41, 127.62, 126.00, 125.44, 125.32, 123.85, 120.27, 119.83, 110.40, 99.12, 94.48, 56.30, 55.73, 23.86, 21.66. MS (FAB): m/z 551.3 [M^+]. Anal. Calcd. $C_{38}H_{38}N$: C, 82.75; H, 6.94; N, 2.54. Found: C, 82.63; H, 6.83; N, 2.71.

Spectral Data of **CzPBM-3**: ^{1}H NMR (400 MHz, $CDCl_3$, 298 K): δ 7.69 (d, *J* = 7.8 Hz, 1H), 7.61 (d, *J* = 8.3 Hz, 2H), 7.54 (d, *J* = 2.5 Hz, 1H), 7.38 (d, *J* = 8.3 Hz, 2H), 7.20 – 7.14 (m, 2H), 7.01 (dd, *J* = 8.9, 2.5 Hz, 1H), 6.88 (d, *J* = 7.9 Hz, 1H), 6.84 (s, 4H), 3.92 (s, 3H), 3.62 (s, 3H), 2.31 (s, 6H), 2.08 (s, 12H). ^{13}C NMR (100 MHz, $CDCl_3$): δ 154.44, 147.06, 142.93, 141.87, 140.96, 138.91, 136.81,

136.48, 130.67, 128.42, 127.69, 125.67, 124.13, 120.23, 115.36, 113.15, 111.15, 108.37, 103.06, 56.42, 55.83, 23.87, 21.67. MS (FAB): m/z 551.3 [M^+]. Anal. Calcd. for $C_{38}H_{38}N$: C, 82.75; H, 6.94; N, 2.54. Found: C, 82.66; H, 7.07; N, 2.58.

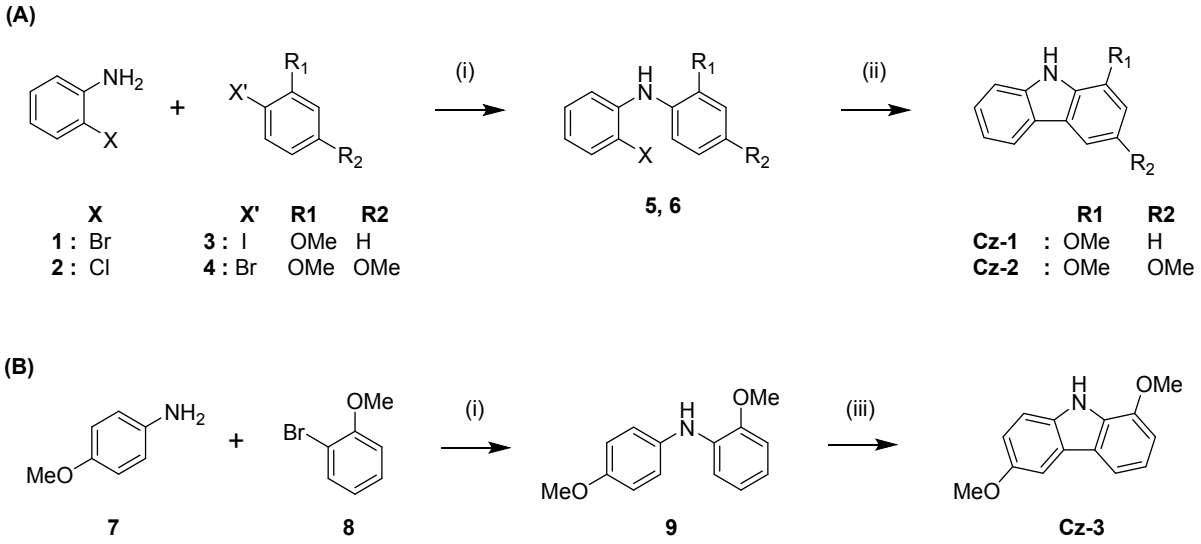

Scheme S1. Synthetic routes of (A) Cz-1 and Cz-2 and (B) Cz-3. Experimental conditions: (i) ^{t}BuONa, Pd_2dba_3, dppf, toluene, reflux, 24 h. (ii) K_2CO_3, $Pd(OAc)_2$, $P(^{t}Bu)_3$, toluene/DMAc, reflux, 24 h. (iii) pivalic acid, K_2CO_3, 110 °C, 12 h.

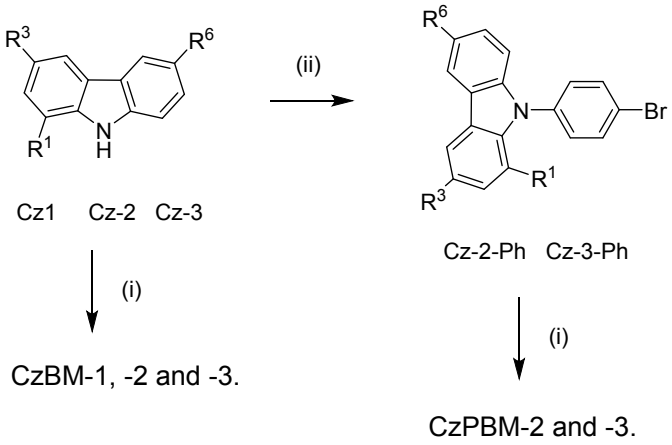

Scheme S2. Synthetic routes of **CzBM-1**, **2** and **3** and **CzPBM-2** and **3**. Experimental conditions: (i) a) *n*-BuLi, THF, −78 °C, 1 h. b) $(Mes)_2BF$, warm to RT, reflux 12 h; (ii) 1-bromo-4-iodobenzene, Cu powder, K_2CO_3, DMF, Reflux, 24 h.

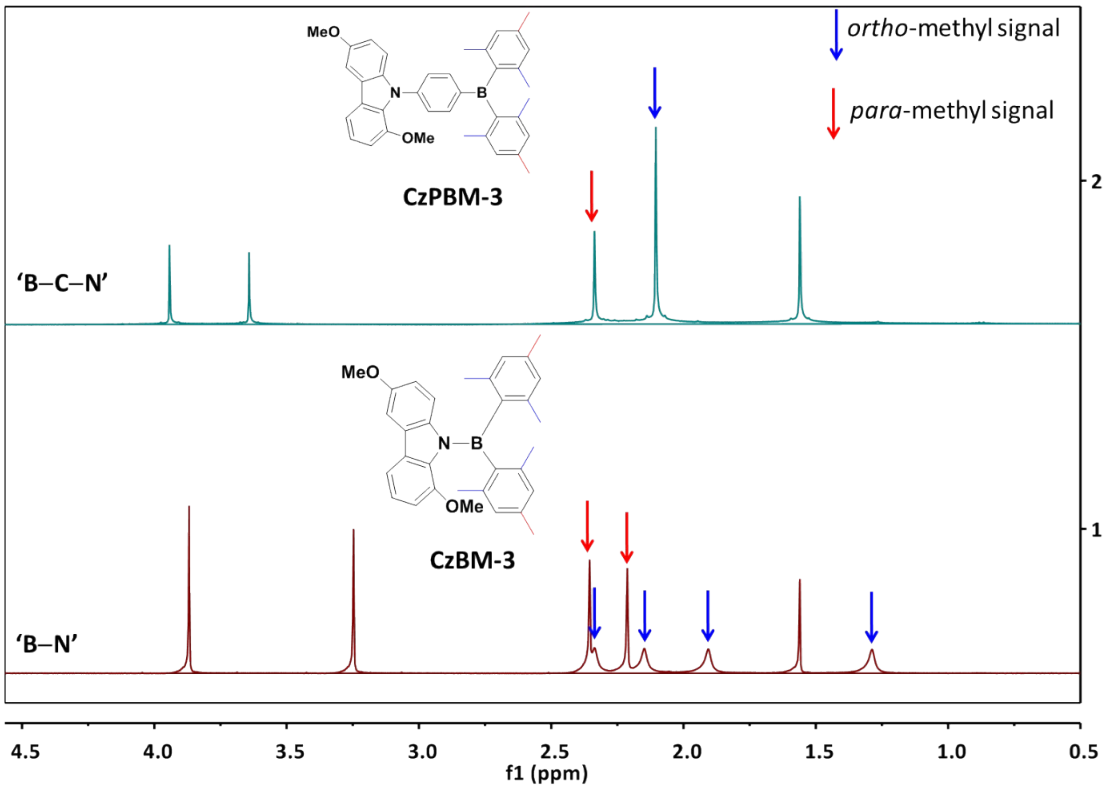

Figure S1. ^{1}H NMR spectra displaying the '*ortho*' and '*para*' – methyl proton signals of mesityl unit in CzBM-3, and CzPBM-3. This *ortho*' and '*para*' methyl proton signals is marked with blue and red colored downward arrow symbols respectively. The distinct pattern of these methyl protons between the B-N and B–C_6H_4–N compounds is due to the restricted rotation of the mesityl unit in the former type compounds.

3. Thermogravimetric analysis (TGA) Methods:

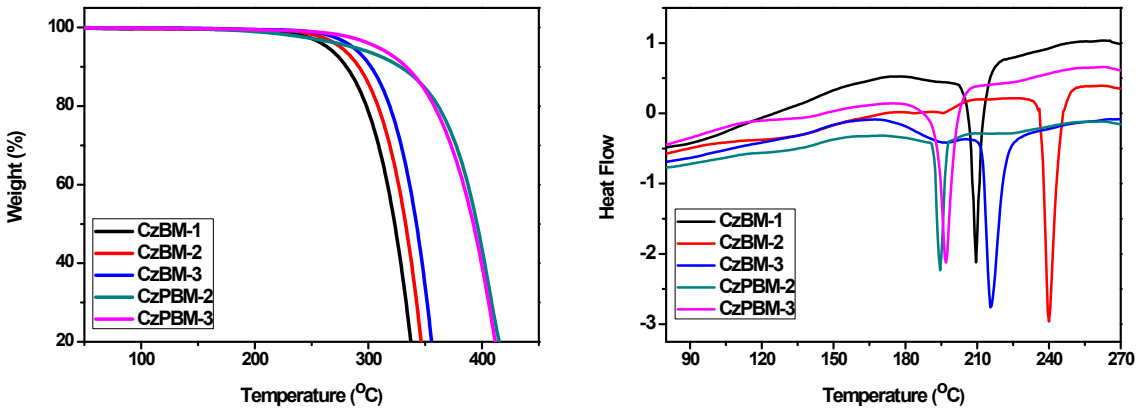

Figure S2. TGA (left) and DSC (right) data of **CzBM-1 to 3, CPBM-2 and 3**. The samples were heated under a nitrogen atmosphere at a heating rate of 10 °C/min

Table S1. Thermal analysis of **CzBM-1 to 3, CPBM-2 and 3**.[a]

	CzBM-1	**CzBM-2**	**CzBM-3**	**CzPBM-2**	**CzPBM-3**
T_d (°C)[b]	264	276	286	287	308
T_g (°C)	192	196	195	136	141
T_m (°C)	210	240	216	195	197

[a] T_d, T_g, and T_m represent the decomposition temperatures, glass transition, and melting temperatures respectively. [b] Temperature at 5% weight loss to initial weight.

4.Photophysical properties:

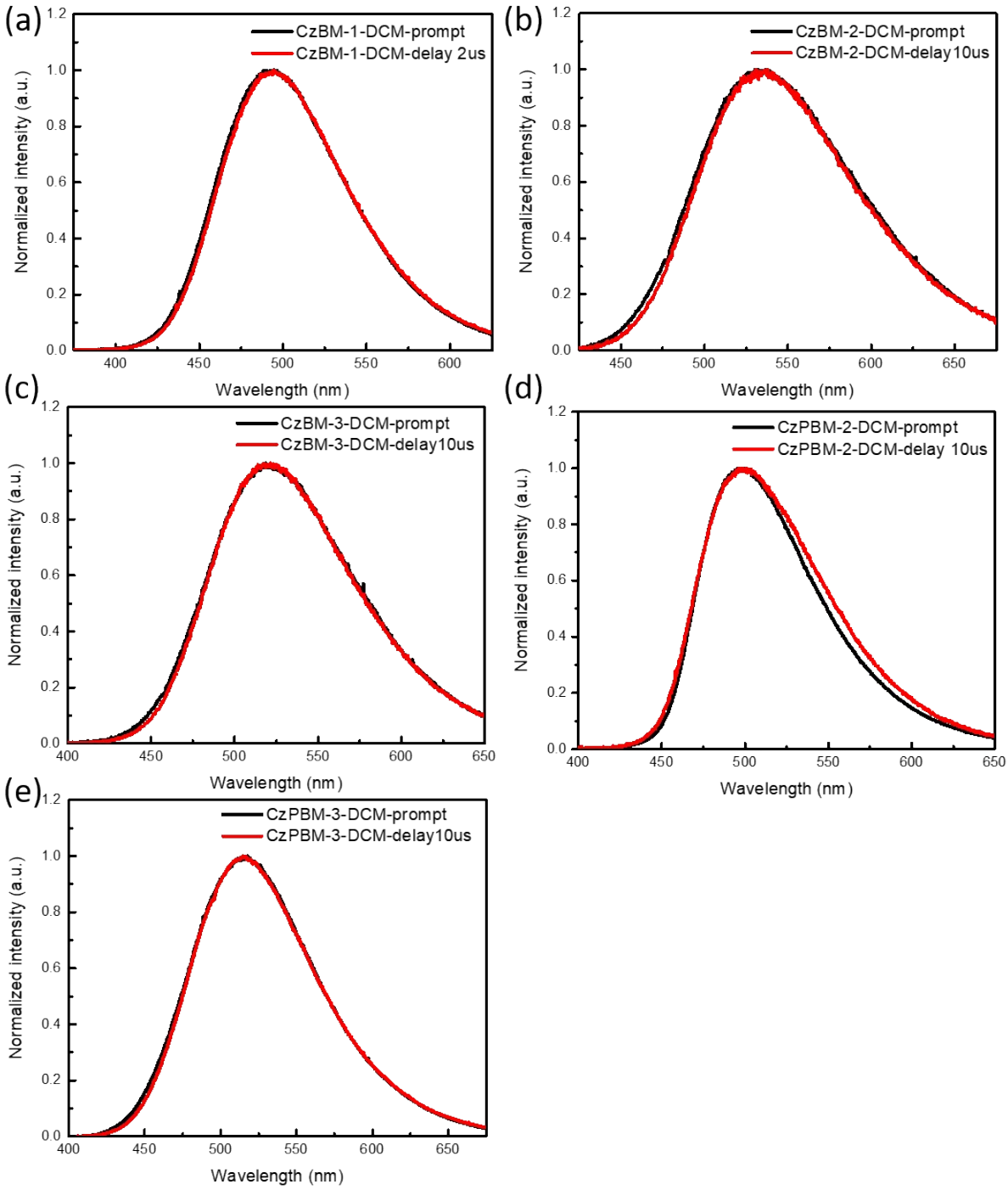

Figure S3. The time resolved PL spectra of the titled molecules in CH_2Cl_2 solution, (a) **CzBM-1**, (b) **CzBM-2**, (c) **CzBM-3**, (d) **CzPBM-2** and (e) **CzPBM-3**. Prompt (black line: delay = 0 ns, gate width = 50 ns) and delayed (red line: delay time as described in the figure, gate width = 10 μs) components of PL spectra.

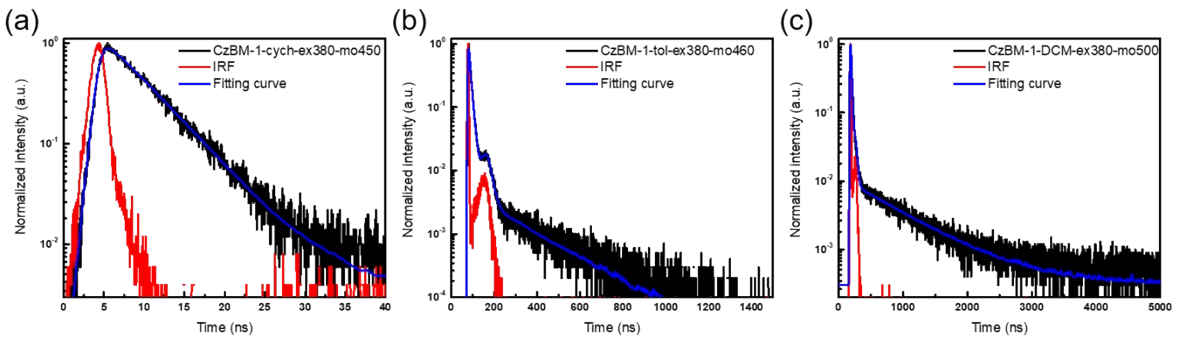

Figure S4. Transient photoluminescence characteristics of the **CzBM-1** in CH_2Cl_2 solutions. Notes that the excitation and monitored wavelengths are descripted in the figure. IRF represents the instrument response function (red).

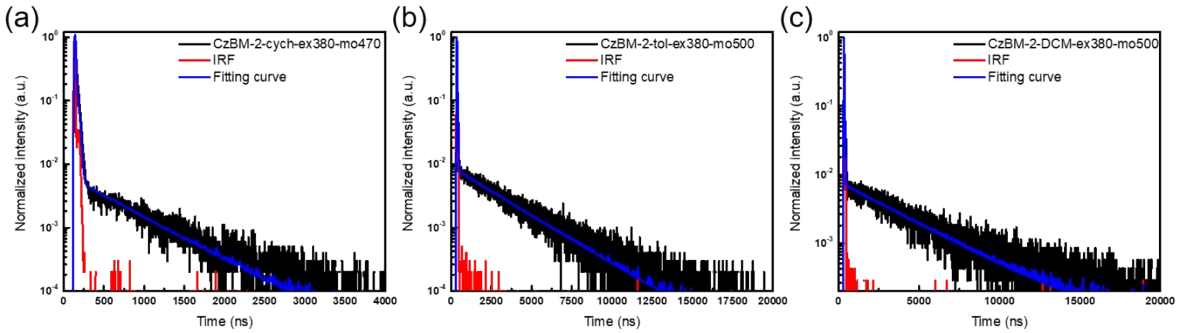

Figure S5. Transient photoluminescence characteristics of the **CzBM-2** in CH_2Cl_2 solutions. Notes that the excitation and monitored wavelengths are descripted in the figure. IRF represents the instrument response function (red).

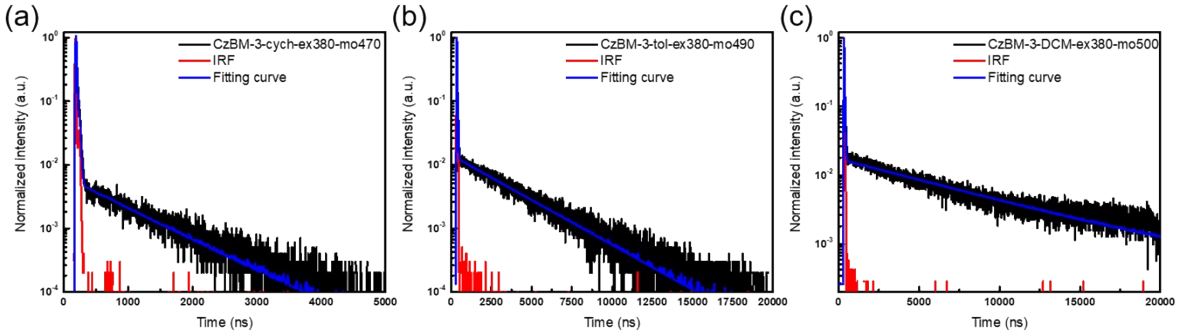

Figure S6. Transient photoluminescence characteristics of **CzBM-3** in CH_2Cl_2 solutions. Notes that the excitation and monitored wavelengths are descripted in the figure. IRF represents the instrument response function (red).

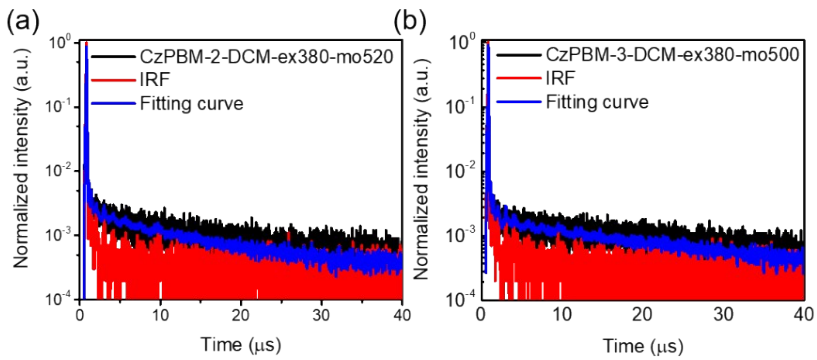

Figure S7. Transient photoluminescence characteristics of **CzPBM-2** and **3** in CH_2Cl_2 solutions. Notes that the excitation and monitored wavelengths are descripted in the figure. IRF represents the instrument response function (red).

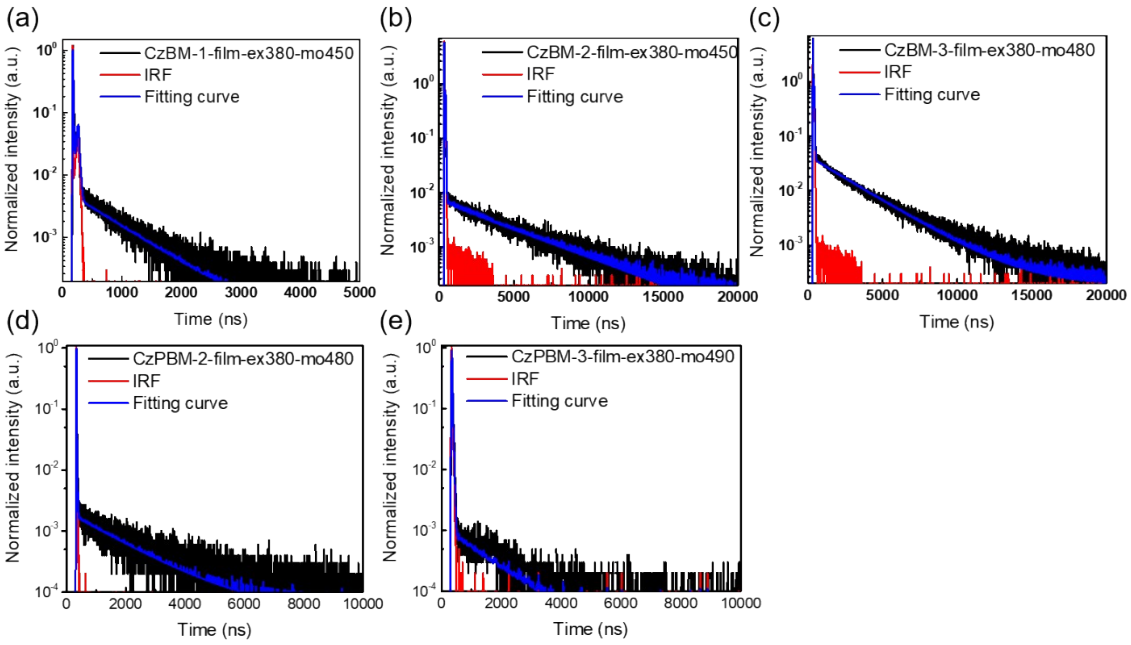

Figure S8. Transient photoluminescence characteristics of the titled molecules in neat film. Notes that the monitored wavelengths are descripted in the figure. IRF represents the instrument response function (red).

Table S2. Photophysical properties of the studied boron compounds under various states at room temperature and the calculated K_{isc} and K_{risc}.

	state	λ_{em} [nm]	$\tau_{1,2}$ [ns] and pre-exp. factor $A_{1,2}$	K_{isc} (s^{-1})[a]	K_{risc} (s^{-1})[a]
CzBM-1	cyclohexane	440	4.19 (1)	-	-
	toluene	462	9.8 (0.996), 212(0.004)	2.38×10^8	9.55×10^5
	CH_2Cl_2	480	14.57 (0.998), 764 (0.002)	1.02×10^8	2.04×10^5
	Neat film	442	5.97 (0.999), 721.4 (0.001)	6.86×10^7	6.86×10^4
CzBM-2	cyclohexane	475	10.98 (0.997), 629(0.003)	9.08×10^7	2.73×10^5
	toluene	501	15.29 (0.992), 2840 (0.008)	6.49×10^7	5.23×10^5
	CH_2Cl_2	524	11.53 (0.998), 3520 (0.002)	8.66×10^7	1.73×10^5
	Neat film	481	1.13 (0.997), 4259 (0.003)	8.82×10^8	2.65×10^6
	DPEPO doped film	478	4.94 (0.999), 26633 (0.001)	2.02×10^8	2.02×10^5
CzBM-3	cyclohexane	467	9.98 (0.997), 868 (0.003)	9.99×10^7	3.01×10^5
	toluene	492	15.48 (0.997), 3087 (0.003)	6.44×10^7	1.94×10^5
	CH_2Cl_2	510	20.77 (0.997), 6955 (0.003)	4.80×10^7	1.44×10^5
	Neat film	479	3.58 (0.992), 2657 (0.008)	2.77×10^8	2.23×10^6
	DPEPO doped film	476	8.47 (0.999) 5578 (0.001)	1.18×10^8	1.18×10^5
CzPBM-2	cyclohexane	417	6.42 (1)	-	-
	toluene	464	16.40 (0.998), 10000 (0.002)	6.09×10^7	1.22×10^5
	CH_2Cl_2	519	18.42 (0.998), 10008 (0.002)	5.42×10^7	1.09×10^5
	Neat film	475	12.31 (0.999), 1609 (0.001)	8.12×10^7	8.12×10^4
	DPEPO doped film	474	18.11 (0.999), 2218 (0.001)	5.52×10^7	5.52×10^4
CzPBM-3	cyclohexane	406	5.65 (0.999), 10000 (0.001)	1.77×10^8	1.77×10^5
	toluene	452	12.59 (0.999), 5582 (0.001)	7.93×10^7	7.94×10^4
	CH_2Cl_2	499	21.81 (0.998), 19277 (0.002)	4.58×10^7	9.17×10^4
	Neat film	463	12.49 (0.997), 1251 (0.003)	7.98×10^7	7.98×10^7
	DPEPO doped film	458	31.00 (0.997), 9880 (0.003)	3.22×10^7	9.68×10^4

[a]Notes that the K_{isc} and K_{risc} are calculated from the kinetic factor of τ_1 and τ_2 in the transient PL decay and the equation are shown below. The subscripts p and d indicates prompt and delay transient signals, respectively. The transient photoluminescence figures were fitted and analyzed by the following equation:

$$I(t) = A_1 \exp\left(-{}^{t}/_{\tau_1}\right) + A_2 exp(-{}^{t}/_{\tau_2}) \quad (1)$$

$$K_p = (\tau_1)^{-1}, \; K_d = (\tau_2)^{-1} \quad (2)$$

$$K_{eq} = \frac{K_{isc}}{K_{risc}} = \frac{K_{fast}}{K_{slow}} = \frac{A_1}{A_2} \quad (3)$$

$$K_{isc} + K_{risc} = (\tau_1)^{-1} \quad (4)$$

$$\Delta E_{TS} = -RT\ln(K_{eq}/3) \quad (5)$$

5. Cyclic Voltammograms studies:

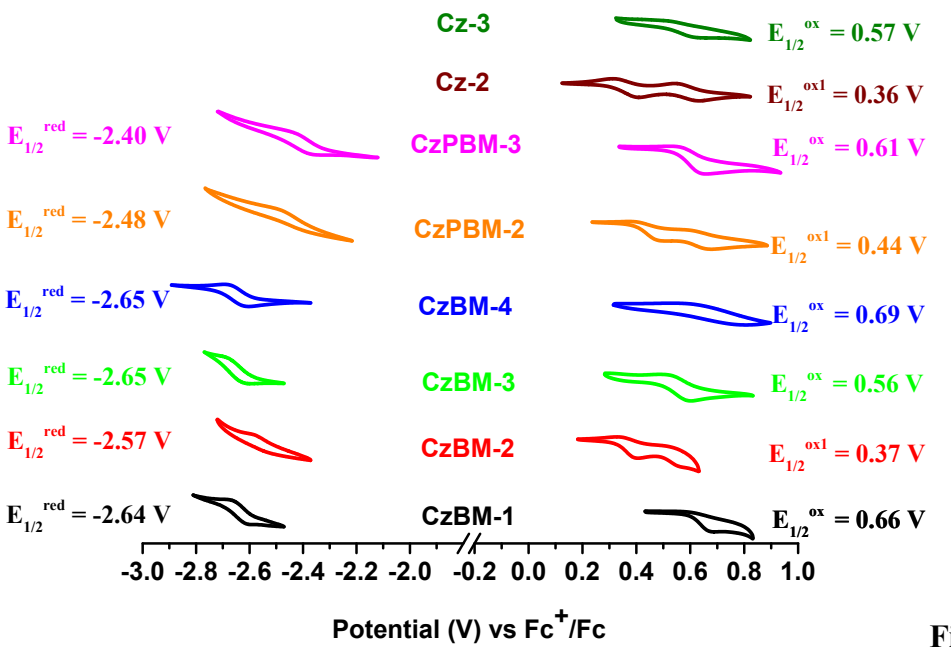

Figure S9. Cyclic voltammograms of Cz-2 and Cz-3, **CzBM-1** to **3**, and **CPBM-2** and **3**. The oxidation and reduction experiments were conducted in acetonitrile solution. The platinum and gold were selected as the working electrode for oxidation and reduction processes, respectively.

Table S3. Electrochemical properties and calculated bandgaps of parent carbazoles Cz-2 and Cz-3 and corresponding TADF molecules.

SAMPLE CODE	$E_{1/2}^{ox}$ (V)[a]	$E_{1/2}^{red}$ (V)[a]	HOMO (eV) CV[b]	LUMO (eV) CV[b]
Cz-2	0.36		–5.16	
Cz-3	0.57		–5.37	
CzBM-1	0.66	–2.64	–5.46	–2.16
CzBM-2	0.37	–2.57	–5.17	–2.23
CzBM-3	0.56	–2.65	– .36	–2.15
CzPBM-2	0.44	–2.48	–5.24	–2.32
CzPBM-3	0.61	–2.40	–5.41	–2.40

[a] $E_{1/2}^{ox}$ and E_{pc}^{re} are the anodic and cathodic peak potentials referenced to the Fc^{+}/Fc couple. [b] HOMO = | –4.8 – $E_{1/2}^{ox}$|, LUMO = | –4.8 – E_{pc}^{re}|.

6. Computational approaches:

Table S4. Calculated wavelength (λ), oscillator strength (*f*) and orbital transition analyses for **CzBM-1** in ground state (R) optimized structure.

Name	λ_{cal}	*f*	assignments	
CzBM-1	316.16	0.2193	HOMO-1→LUMO	(2.23%)
			HOMO→LUMO	(87.17%)
	280.89	0.1997	HOMO-4→LUMO	(5.81%)
			HOMO-3→LUMO	(2.70%)
			HOMO-2→LUMO	(77.79%)
			HOMO-1→LUMO	(2.67%)
			HOMO→LUMO+1	(4.11%)
	279.58	0.0707	HOMO-2→LUMO	(4.05%)
			HOMO-1→LUMO	(2.75%)
			HOMO-1→LUMO	(2.27%)
			HOMO-1→LUMO	(3.25%)
			HOMO→LUMO+1	(79.08%)

Table S5. Calculated wavelength (λ), oscillator strength (*f*) and orbital transition analyses for **CzBM-1** in excited state optimized structure.

Name	λ_{cal}	*f*	assignments	
CzBM-1	372.96	0.0576	LUMO→HOMO	(92.00%)

Table S6. Calculated wavelength (λ), oscillator strength (*f*) and orbital transition analyses for **CzBM-2** in ground state (R) optimized structure.

Name	λ_{cal}	*f*	assignments	
CzBM-2	310.68	0.2798	HOMO→LUMO	87.01%
	270.56	0.0423	HOMO→LUMO+1	87.01%
	270.56	0.2092	HOMO-4→LUMO	3.12%
			HOMO-3→LUMO	8.24%
			HOMO-2→LUMO	64.19%
			HOMO-1→LUMO	15.57%

Table S7. Calculated wavelength (λ), oscillator strength (*f*) and orbital transition analyses for **CzBM-2** in excited state optimized structure.

Name	λ_{cal}	*f*	assignments	
CzBM-2	439.93	0.0478	LUMO→HOMO	(94.23%)

Table S8. Calculated wavelength (λ), oscillator strength (*f*) and orbital transition analyses for **CzBM-3** in ground state (R) optimized structure.

Name	λ_{cal}	*f*	assignments	
CzBM-3	311.79	0.2426	HOMO-1→LUMO	4.11%
			HOMO→LUMO	86.14%
	287.77	0.062	HOMO→LUMO+1	88.32%
	270.39	0.1909	HOMO-4→LUMO	9.45%
			HOMO-2→LUMO	4.11%

Table S9. Calculated wavelength (λ), oscillator strength (*f*) and orbital transition analyses for **CzBM-3** in excited state optimized structure.

Name	λ_{cal}	*f*	assignments	
CzBM-3	434.25	0.0339	LUMO→HOMO	(93.40%)

Table S10. Calculated wavelength (λ), oscillator strength (*f*) and orbital transition analyses for **CzPBM-0** in ground state optimized structure.

Name	λ_{cal}	*f*	assignments	
CzPBM-0	323.11	0.5565	HOMO-7→LUMO	(3.18%)
			HOMO-3→LUMO	(11.83%)
			HOMO→LUMO	(76.16%)
			HOMO→LUMO+1	(2.36%)
	310.19	0.1473	HOMO-11→LUMO	(3.30%)
			HOMO-2→LUMO	(90.89%)
	287.60	0.0004	HOMO-10→LUMO	(2.87%)
			HOMO-3→LUMO	(77.70%)
			HOMO→LUMO	(11.05%)

Table S11. Calculated wavelength (λ), oscillator strength (*f*) and orbital transition analyses for **CzPBM-2** in ground state optimized structure.

Name	λ_{cal}	*f*	assignments	
CzPBM-2	331.73	0.4684	HOMO-3→LUMO	(7.30%)
			HOMO→LUMO	(79.29%)
			HOMO-4→LUMO+1	(2.07%)
	308.43	0.1545	HOMO-11→LUMO	(3.50%)
			HOMO-2→LUMO	(90.72%)
	299.31	0.0615	HOMO→LUMO+1	(88.34%)
	289.52	0.0405	HOMO-10→LUMO	(3.59%)
			HOMO-3→LUMO	(80.19%)
			HOMO→LUMO	(7.35%)
	274.66	0.0294	HOMO-5→LUMO	(4.00%)
			HOMO-4→LUMO	(81.32%)
	273.65	0.0396	HOMO-5→LUMO	(80.62%)
			HOMO-4→LUMO+1	(3.97%)

Table S12 Calculated wavelength (λ), oscillator strength (*f*) and orbital transition analyses for **CzPBM-2** in excited state optimized structure.

Name	λ_{cal}	*f*	assignments	
CzPBM-2	380.85	0.4084	LUMO→HOMO	(88.65%)

Table S13. Calculated wavelength (λ), oscillator strength (*f*) and orbital transition analyses for **CzPBM-3** in ground state optimized structure.

Name	λ_{cal}	*f*	assignments	
CzPBM-3	331.66	0.4767	HOMO-3→LUMO	(6.70%)
			HOMO-1→LUMO	(2.28%)
			HOMO→LUMO	(78.17%)
	308.26	0.1532	HOMO-2→LUMO	(90.17%)
	299.95	0.0761	HOMO-1→LUMO+1	(88.12%)
	289.84	0.0413	HOMO-3→LUMO	(77.72%)
			HOMO-1→LUMO	(2.22%)
			HOMO→LUMO	(8.27%)
	274.68	0.0335	HOMO-6→LUMO	(10.69%)
			HOMO-5→LUMO+1	(71.41%)
			HOMO-4→LUMO+1	(2.92%)

Table S14. Calculated wavelength (λ), oscillator strength (*f*) and orbital transition analyses for **CzPBM-3** in excited state optimized structure.

Name	λ_{cal}	*f*	assignments	
CzPBM-3	369.56	0.5110	LUMO→HOMO	(86.10%)

Table S15. Calculated orbital energy levels' for the titled molecules.[a]

Name	HOMO-3	HOMO-2	HOMO-1	HOMO	LUMO[b]
CzBM-1	-7.760	-7.629	-7.323	-6.945	-3.024
CzBM-2	-7.762	-7.638	-7.262	-6.797	-2.807
CzBM-3	-7.760	-7.627	-7.333	-6.786	-2.810
CzPBM-0	-7.759	-7.661	-7.350	-6.873	-3.036
CzPBM-2	-7.710	-7.618	-7.218	-6.479	-2.742
CzPBM-3	-7.712	-7.612	-7.238	-6.489	-2.751

[a] Notes that the energy levels were recorded in an unit of eV. [b] Notes that the LUMO were calculated from the lowest lying absorption energy gap added the corresponding HOMO level.